Chapter 12

DNA-Directed Antibody Immobilization for Robust Protein Microarrays: Application to Single Particle Detection 'DNA-Directed Antibody Immobilization

Nese Lortlar Ünlü*, Fulya Ekiz Kanik*, Elif Seymour, John H. Connor, and M. Selim Ünlü

Abstract

Protein microarrays are emerging tools which have become very powerful in multiplexed detection technologies. A variety of proteins can be immobilized on a sensor chip allowing for multiplexed diagnostics. Therefore, various types of analyte in a small volume of sample can be detected simultaneously. Protein immobilization is a crucial step for creating a robust and sensitive protein microarray-based detection system. In order to achieve a successful protein immobilization and preserve the activity of the proteins after immobilization, DNA-directed immobilization is a promising technique. Here, we present the design and the use of DNA-directed immobilized (DDI) antibodies in fabrication of robust protein microarrays. We focus on application of protein microarrays for capturing and detecting nanoparticles such as intact viruses. Experimental results on Single-particle interferometric reflectance imaging sensor (SP-IRIS) are used to validate the advantages of the DDI method.

Key words Protein microarrays, DNA-directed antibody immobilization, Label free detection, Single particle detection, SP-IRIS

1 Introduction

Protein microarrays have become indispensable tools with a wide variety of applications including biomarker detection, protein-protein interaction analysis, and detection of small molecule targets as in drug discovery [1, 2]. They are also promising candidates for multiplexed clinical diagnostics and disease progression monitoring [3]. Here, we first describe the challenges of protein microarrays to motivate DNA-directed antibody immobilization (DDI) for production of robust protein microarrays. For characterization

*These authors contributed equally to this work.

Avraham Rasooly and Ben Prickril (eds.), *Biosensors and Biodetection: Methods and Protocols Volume 1: Optical-Based Detectors*, Methods in Molecular Biology, vol. 1571, DOI 10.1007/978-1-4939-6848-0_12,

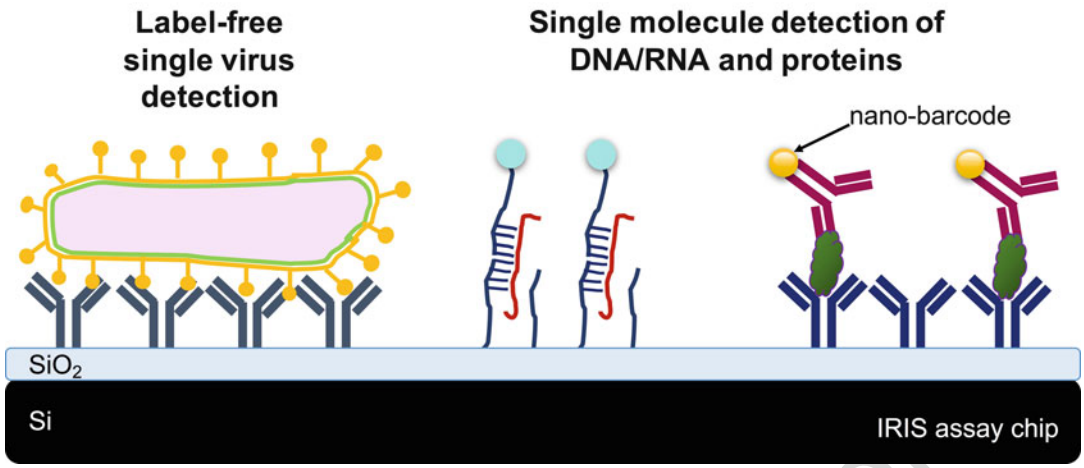

Fig. 1 Conceptual representation of IRIS detection platform for digital detection of individual viral particles and antigens labeled with gold nanoparticles

of the protein microarrays, we use Interferometric Reflectance Imaging Sensor (IRIS) technology developed in our laboratory. The IRIS platform has two distinct operation modalities [4]: (1) high-throughput label-free measurement of biomass accumulation; and (2) digital detection of single particles with high-magnification, also known as Single Particle Interferometric Reflectance Imaging Sensor (SP-IRIS). First modality is utilized for label-free characterization of probe immobilization and the latter is used for comparison of protein chips for single particle (virus) detection applications. Figure 1 shows the detection of single virus particles and single molecule detection of proteins and DNA/RNA, conceptually. With SP-IRIS, particles, which are too small to be detected by the standard microscopy, such as viruses, can be easily detected, quantified and differentiated according to their size and shape. Moreover, it becomes possible to detect individual molecules, such as proteins and DNA, via labeling with small metallic nanoparticles with high sensitivity [4].

The high-throughput protein microarrays are based on the technology developed for DNA chips that made profound impact in genomic analysis. Fabrication of DNA chips benefit from the ease of uniform immobilization of DNA probes on the sensor surface. DNA probes of different sequences can be chemically functionalized at a particular end (e.g. amine, thiol, or carboxyl functionalization) or have identical regions in the proximity of the solid sensor surface to assure uniformity. In contrast, proteins represent a great diversity of size and conformation resulting in significant variability of surface immobilization. Therefore, despite many advantages of protein microarrays in proteomics and multiplexed diagnostics applications, the technical difficulties associated with fabrication

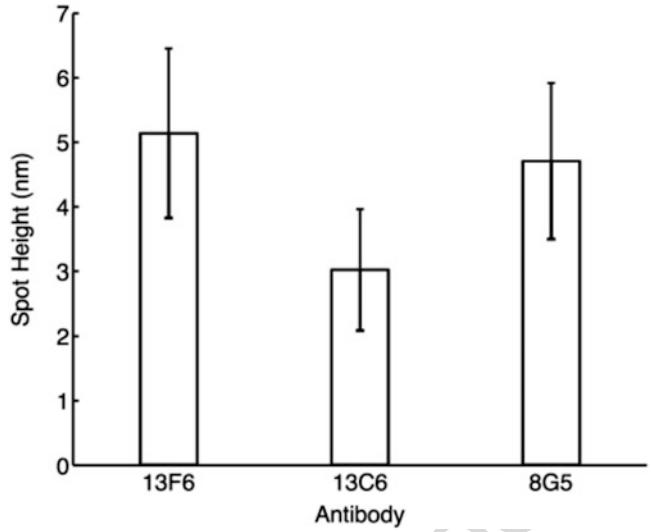

Fig. 2 Variation of antibody immobilization for different types of antibodies. In this particular example, we compare 13F6 (anti-EBOV glycoprotein antibody), 13C6 (anti-EBOV glycoprotein antibody) and 8G5 (anti-wild type VSV glycoprotein antibody) were used. Error bars show the variation among 60 different spots in ten different spotting runs

and reliability of the protein chips limit the potential of this promising technology. Perhaps the most fundamental challenge to overcome is related to the immobilization of proteins on the microarray surface in a repeatable manner. Furthermore, how the proteins are bound on the surface as well as the orientation of the protein probes significantly affects their capture efficiency. For example, on an amine-reactive sensor surface, the protein probes may have multiple covalent interactions that limit their accessibility to bind to a target molecule [5]. Moreover, challenges such as variability of spot properties and protein immobilization within and across chips influence the accuracy and robustness of protein microarrays. As illustrated in Fig. 2, when different types of antibodies are spotted, a significant difference in spot heights (as characterized by IRIS), thus a variation in antibody surface densities, is observed.

In this chapter, we describe DNA-directed antibody immobilization (DDI) for robust protein microarrays specifically for applications in single particle (or digital) detection - an exciting recent technological development that provides sensitivity beyond the reach of ensemble measurements [6–8] but brings along additional challenges. We have demonstrated an optical imaging technique termed Single-Particle Interferometric Reflectance Imaging Sensor (SP-IRIS)—a versatile platform that allows for a large range of nanoparticle detection including both natural nanoparticles (such as viruses) and synthetic nanoparticles in a highly-multiplexed

microarray format [9]. The technology is based on interference of light from an optically transparent multi-layer dielectric structure. The interference of light reflected from the sensor surface is modified by the presence of particles producing a distinct signal that reveals the presence and size of the particle that is not otherwise visible under a conventional microscope. Size discrimination of the imaged virions in label-free virus detection allows for rejection of non-specifically bound particles to achieve a limit-of-detection competitive with the state-of-the-art laboratory technologies [10]. SP-IRIS has also shown promising results for detection of protein [11] and DNA molecules labeled with small gold nanoparticles—showing attomolar sensitivity and meeting the requirements for most in vitro tests.

Using our experimental results on digital detection of viruses via SP-IRIS, we illustrate the additional and more stringent requirements for robust protein microarrays. For a typical molecular detection assay, (for example when protein probes are used to capture protein biomarker targets), the signal is expected to vary linearly with the probe density. Therefore, assay variability due to probe immobilization differences can be accounted for and calibrated as described in [12]. In detection of intact viruses (or nanoparticles much larger than individual protein molecules), the influence of probe density is much more significant as illustrated by the experimental results in Fig. 3. The amount of virus that is captured on the antibody spots increases rapidly with the surface antibody density. Also, virus capture nearly vanishes when probe density drops below 5×10^9 Ab/mm^2 corresponding to less than 20% surface coverage.

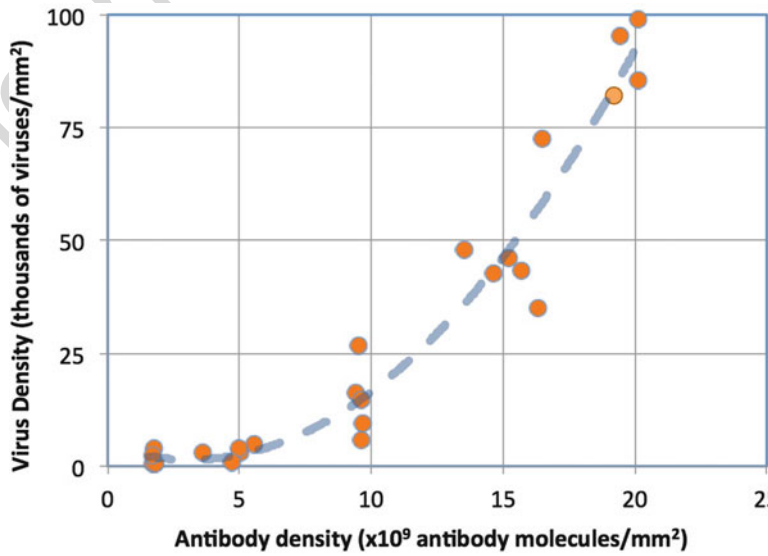

Fig. 3 The dependence of virus capture on the density of antibody immobilization on the sensor surface illustrating the strong variation

We speculate that multiple antibody-antigen binding interactions are required for the capture of viruses. A sparse coverage of immobilized antibodies on a solid surface does not allow for multiple interactions with the proteins on the relatively rigid surface of the target virus resulting in significant reduction of capture efficiency. One potential solution is to attach the antibodies to the sensor surface with flexible tethers thus allowing them to conform to the surface of the virus to make multiple bonds even for relatively sparse surface coverage. This is precisely the most significant motivation for using DNA-directed antibody immobilization in the context of single particle (such as an intact virus) detection.

Motivated by the limitations of direct immobilization of antibodies, various alternative methods have been explored for protein immobilization to promote antibody activity and improve assay sensitivity. DNA-directed immobilization (DDI), one of the recent alternative methods for protein immobilization, combines both the robustness of DNA microarrays with the diagnostic utility of proteins through the use of protein-DNA conjugates to functionalize a DNA surface for subsequent antigen capture [13–15]. Previous studies demonstrated that DDI enhanced molecular (antigen) capture efficiency, refined spot homogeneity and improved assay reproducibility contrasted to direct covalent immobilization of antibodies on the solid surface [16–18]. To validate the improved capture efficiency in the context of single particle detection, we have compared DDI to direct antibody immobilization [19]. A systematic study demonstrated that antibodies attached to the sensor surface with flexible tethers (DNA) provide additional conformational freedom, elevate the capture probes from the solid sensor surface and increases the target capture efficiency. Therefore, DDI not only provides a more robust protein microarray fabrication process directly benefiting from well-established DNA chips but also enhances sensitivity. Additional advantages of DNA-directed antibody immobilization include the ability to reprogram the sensor surface by using a different set of antibodies conjugated to the same DNA sequences and the resilience of DNA microarrays in elevated temperatures required for assembly of microfluidic cartridges [19]. In DDI, selected antibodies are covalently attached to specific DNA sequences which are complementary to surface probe ssDNA sequences. The surface probe sequences are immobilized onto the sensor surface and antibody-attached DNA sequences hybridize to the surface probes on the surface [19] as represented in Fig. 4.

Below, we describe the detailed method for DNA-directed immobilization of antibodies and application to single virus detection. We illustrate the advantages using experimental results on SP-IRIS platform.

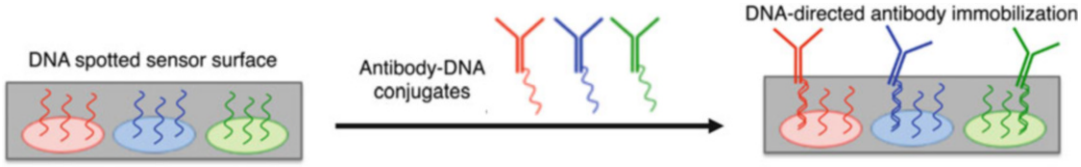

Fig. 4 A schematic representation of SP-IRIS substrate surface with ssDNA spots and the conversion of the DNA chip into a triplex antibody array through DDI of antibodies. Reprinted with permission from Seymour et al. Anal. Chem., 2015, 87 (20), pp. 10505–10,512. Copyright 2016 American Chemical Society

2 Materials

2.1 Single-Particle Interferometric Reflectance Imaging Sensor (SP-IRIS) (Validation Platform: Can Be Replaced by Another Single Particle Detection Method)

1. Scientific CCD camera. Retiga 4000R (Qimaging, Corp., Surrey, BC, Canada).
2. Sample illumination source. 530 nm LED source (Thorlabs Inc., Newton, NJ, USA).
3. Microscope objectives. 50× 0.8 NA Nikon objective for dry samples or a 40× 0.9 NA Nikon objective for samples in liquid (Nikon Inc., Melville, NY, USA) (*see* **Note 1**).
4. CRISP (The Continuous Reflection Interface Sampling and Positioning) autofocus system. MFC-2000 (Applied Scientific Instrumentation, Eugene, OR, USA).
5. 50:50 Beam splitter (Thorlabs Inc., Newton, NJ, USA).
6. Lenses (Thorlabs Inc., Newton, NJ, USA). Achromatic doublets for the visible spectrum. Catalogue numbers: f_1: AC254-030-A-ML, f_2: AC254-050-A-ML and f_3: AC254-200-A-ML.
7. Diffuser (Thorlabs Inc., Newton, NJ, USA). N-BK7 Ground Glass Diffuser, 220 Grit.
8. XY stage.
9. Mechanical components for optical setup. Cage system and lens holders (Thorlabs Inc., Newton, NJ, USA).
10. Computer. Data acquisition and processing.

2.2 Substrate Fabrication

1. Silicon (Si/SiO_2) chips with a patterned thermally grown silicon dioxide for single particle detection experiments (Silicon Valley Microelectronics, Santa Clara, CA, USA) (*see* **Note 2**).
2. Dimensions of the chips: 10 mm × 10 mm × 0.5 mm, with a 2.3 mm × 2.3 mm active center region for spotting DNA probes.

2.3 Surface Chemistry

1. Copoly(*N*,*N*-dimethylacrylamide (DMA)-acryloyloxysuccinimide (NAS)-3-(trimethoxysilyl)-propylmethacrylate (MAPS)) (Copoly(DMA-NAS-MAPS)) (MCP-2) (Lucidant Polymers Inc., Sunnyvale, CA, USA) (*see* **Note 3**).
2. Solution A2. Coat-On™ Coating buffer (Lucidant Polymers Inc., Sunnyvale, CA, USA).

3. Acetone and isopropanol.
4. Plastic petri dish.
5. Plasma asher.
6. Vacuum drying oven.

2.4 Protein Microarray Preparation

1. HPLC purified 5′-aminated ssDNA molecules (Integrated DNA Technologies, Inc., Coralville, IA, USA). A surface probe and a linker (for antibody conjugation) sequences.
2. Monoclonal antibody. As a model antibody against Ebola virus (EBOV) glycoprotein (13F6) (Mapp Biopharmaceutical Inc., San Diego, CA, USA).
3. DNA spotting buffer (2×): 300 mM sodium phosphate buffer, pH 8.5. 42. 59 g of Na_2HPO_4 and 7.35 g of NaH_2PO_4 is dissolved in 1 L of filtered deionized water (18.2 MΩ resistivity, 0.2 μm-filtered) (Barnstead, NANOpure Diamond water purification system). The pH is adjusted to 8.5 with HCl. Stored at room temperature.
4. Tris–HCl buffer (1×): 50 mM Tris–HCl with 150 mM NaCl, pH 8.5. 6.06 g of Tris is dissolved in 800 mL filtered deionized water. pH is adjusted to 8.5 with the appropriate volume of concentrated HCl. Final volume is brought to 1 L with deionized water. Stored at room temperature.
5. Blocking solution: 50 mM ethanolamine in Tris–HCl buffer. 310 μL of ethanolamine is added to 100 mL of Tris–HCl buffer (*see* **Note 4**).
6. Wash buffer (PBST): PBS buffer with 0.1% Tween-20. Stored at room temperature.
7. Sodium nitrate solution: 0.5 M sodium nitrate. 43 g of $NaNO_3$ is dissolved in 1 L of water.
8. Antibody-DNA conjugation kit (Thunder-Link Oligo Conjugation Kit, Innova Bioscience, Cambridge, UK).
9. Piezoelectric microarray spotter. Scienion S3 Fleaxarrayer (Berlin, Germany).
10. 24-well plate.
11. Multipurpose rotating shaker.
12. For comparison purpose only, antibodies are immobilized directly (*see* **Note 5**).

2.5 In-Liquid Virus Detection (Selected for Validation Experiments: Other Techniques Can Be Substituted)

1. Microfluidic cartridges. Multilayer polymer laminate devices: Disposable, custom-designed (ALine, Inc., Rancho Dominguez, CA, USA). From the bottom pf the costom-designed chip, Layer 1: acrylic, Layer 2: Si-PSA, Layer 3: polycarbonate, Layer 4: PET and Layer 5: PET.

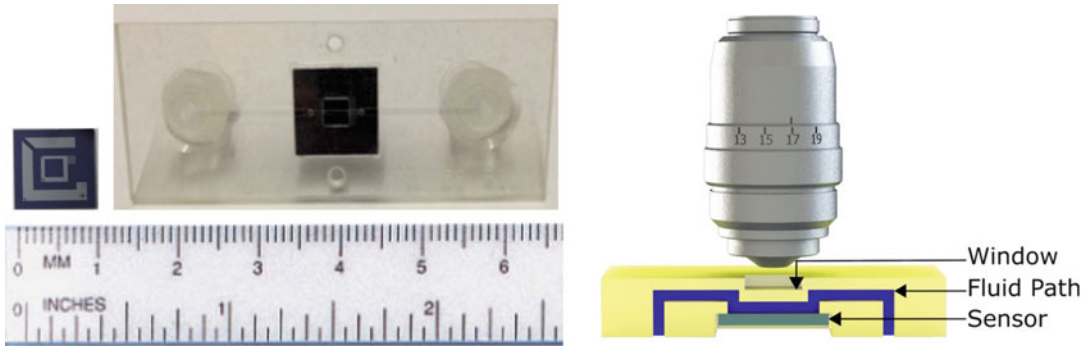

Fig. 5 The images of an SP-IRIS chip and microfluidic cartridge for in-liquid SP-IRIS measurements (on the *left*). Cross section model of the microfluidic cartridge and objective which indicates the fluidic path (in *blue*), the sensor (in *gray*) and the chip and imaging window (in *yellow*) not to scale (on the *right*). Adapted with permission from Sherr et al. ACS Nano, 2016, 10 (2), pp. 2827–2833. Copyright 2016 American Chemical Society

2. Syringe pump. PHD 2000 (Harvard Apparatus, Holliston, MA, USA).
3. Silicon Tubing. FEP Nat 1/16 × 0.010 × 20 ft (Upchurch Scientific, IDEX Health and Science, Middleborough, MA, USA).
4. Adaptors, syringes, fitting.
5. Figure 5 shows an SP-IRIS chip, a microfluidic cartridge and a schematic representation of the imaging setup.

2.6 Data Processing

1. MATLAB (MathWorks, Natick, MA, USA).
2. Custom particle detection software developed in MATLAB.

3 Methods

3.1 DNA Sequence Design

1. DNA sequences are designed to minimize the hairpin, self-dimer and heterodimer structures to increase the hybridization efficiency and prevent cross hybridization (*see* **Note 6**).
2. Twenty base pair of DNA sequence used as the surface probe (40 mer) is complementary to the antibody conjugated sequence used in the antibody-conjugation.
3. Amine modification is introduced at the 5′-end of the surface probe DNA sequence in order to achieve covalent immobilization on the copoly(DMA-NAS-MAPS) polymer coated chip surface. Table 1 shows the DNA sequences used in this work for antibody immobilization.
4. Lyophilized oligonucleotides are dissolved in ultrapure water to have a final concentration of 100 μM. 100 μL aliquots are made. The concentration of the DNA solution is

Table 1 t.1
Model surface probe DNA sequence and its corresponding sequence used in antibody-conjugation in this work

Antibody	DNA sequences conjugated to the antibodies	DNA sequences immobilized on the chip surface	t.2
Anti-EBOV GP (13F6)	B: 5′AAAAATACAGAGTTA GTCGCAGTGG3′	B′: 5′ATCCGACCT TGACATCTCTACCACTGCGACTAACTCTGTA3′	t.3

Complementary sequences are *underlined*. This particular sequences are selected as an example to be used in DNA-directed immobilization t.4

determined spectrophotometrically by measuring the absorbance at 260 nm. The aliquots are stored at −20 °C. When needed, a single aliquot is thawed and used immediately.

3.2 Protein Microarray Fabrication

1. The silicon chips are functionalized with the polymer copoly (DMA-NAS-MAPS). Prior to polymer coating, the chips are cleaned by sonicating in acetone for 5 min, rinsing in isopropanol and deionized water. Then, the chips are dried by blowing nitrogen gas.
2. The chips are cleaned by plasma ashing with oxygen plasma at 300 sccm and 500 W for 10 min.
3. 1% (w/v) copoly(DMA-NAS-MAPS) is dissolved in a mixture of Solution A2 and water (1:1) by vigorous vortexing.
4. The clean chips are placed in a plastic petri dish and the polymer solution is poured onto the chips until they are fully covered with the solution (*see* **Note 7**).
5. The chips are incubated in the polymer solution for 30 min at room temperature while shaking.
6. After functionalization, the chips are rinsed and dipped in deionized water for 3 min with shaking. This is repeated for three times. Then, the chips are dried with nitrogen gas.
7. In a vacuum oven, the chips are baked for 15 min at 80 °C (*see* **Note 8**).
8. To prepare protein microarrays via DNA-directed immobilization technique, surface probe oligonucleotide (Sequence B′) is spotted on the polymer-functionalized chips at an optimum concentration of 30 μM in sodium phosphate buffer (150 mM, pH 8.5). In order to determine the effect of probe density, a varying degree of immobilization for antibody-conjugate was created and virus capture capacity was determined by spotting DNA surface probe at different concentrations which are 3, 6, 12, 18, 24 and 30 μM. Each concentration is spotted in six replicates on the chip (*see* **Note 9**).

9. An automated piezoelectric arrayer is used to spot surface probe DNA. A microarray pattern is designed for six replicate spots for the probe DNA. The space between the spots is set as 288 μm.
10. The humidity and the temperature inside the spotter chamber are set to 67% and 20 °C, respectively (*see* **Note 10**).
11. After spotting, DNA-spotted chips are kept in the spotter chamber at 67% humidity overnight at room temperature.
12. Following the immobilization, the chips are incubated in blocking solution for 30 min to quench the excessive NHS groups left reactive after immobilization.
13. Then, the chips are washed with wash buffer for 30 min while shaking.
14. Afterwards, the chips are rinsed with phosphate buffer saline and deionized water, and dried with nitrogen.
15. Antibody-DNA conjugates are synthesized using Thunder-Link oligo conjugation kit according to manufacturer's protocol. 40 μM 5′-aminated linker DNA (Sequence B) is reacted with 1 mg/mL antibody (13F6) (*see* **Note 11**).
16. Antibody immobilization is achieved by incubating the DNA-chips with the antibody-DNA conjugate solution (at 5 μg/ml in PBS with 1% BSA) for 1 h in a 24-well plate on a shaker.
17. After DNA-DNA hybridization and antibody immobilization, the chips are washed with PBS twice, 0.5 M sodium nitrate solution twice, and then, dipped in cold 0.1 M sodium nitrate solution. Finally, the chips are dried with nitrogen gas.
18. For comparison purpose only, antibodies are immobilized directly (*see* **Notes 12** and **13**).

3.3 Quality Control of the Modified Chips

1. Biomass quantification is performed for direct antibody-immobilized and DNA directed antibody-immobilized chips using IRIS (*see* **Note 14**).
2. To test the activity of DNA conjugate for binding to its target, biomass measurements of the conjugate hybridization and virus binding for both directly immobilized and DNA-tethered antibody are performed. The spots are imaged before antibody-conjugate hybridization, after hybridization (thus, antibody immobilization) and after virus (VSV) capture, shown in Fig. 6. After the immobilization and virus capture, the spot height change is identified with IRIS measurements concluding that although DNA-spots have much less probe density (⅓ of antibody-spot density), they capture almost the same amount of virus with the direct-antibody spots. This shows the significant improvement in the capture efficiency due to DDI for protein immobilization. The height change in

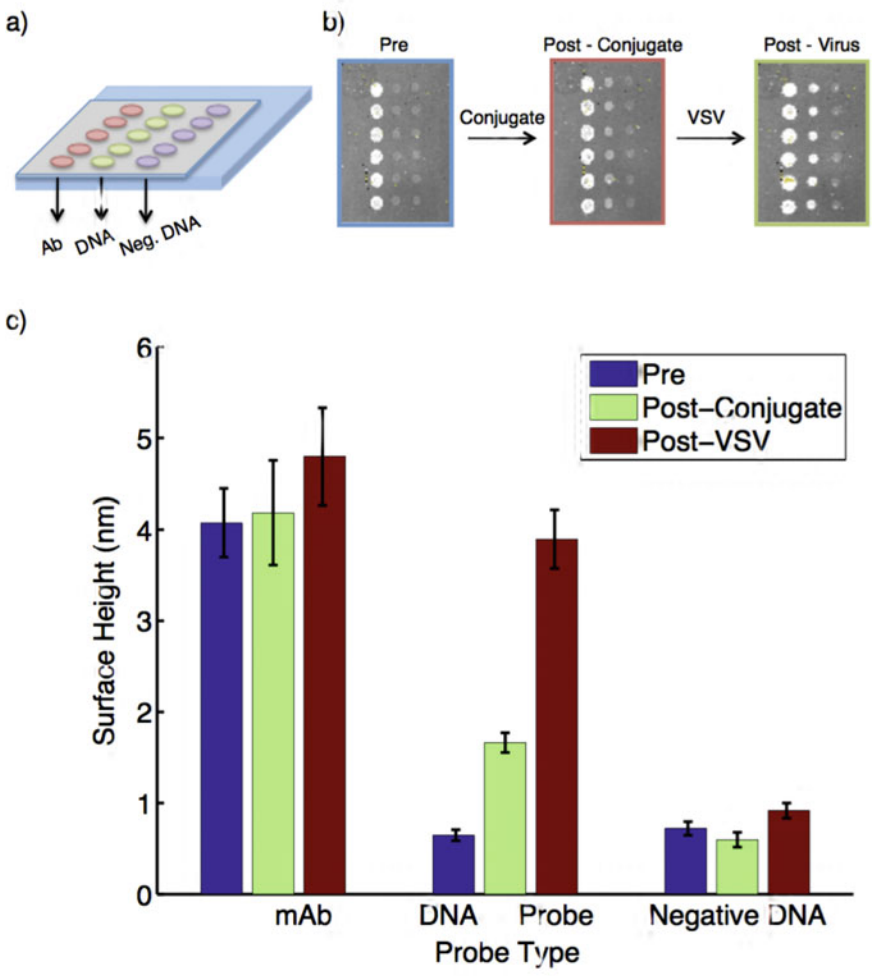

Fig. 6 IRIS average spot height measurements for direct-antibody and DNA-directed immobilized-antibody spots. One nanometer of surface thickness corresponds to 1.2 ng/mm^2 of antibody density. (**a**) Schematic representation of the IRIS chip spotted with three different probe types: antibody, probe DNA and a negative DNA sequence (not complementary to target antibody-conjugated DNA). (**b**) IRIS images of the chip at different stages of the experiment: before hybridization of DNA B-conjugate, after hybridization of the conjugate and after incubating with VSV virus. (**c**) IRIS surface height measurements for three different stages of the experiment

the antibody spots shows that they are only able to capture a small amount of virus even though they are spotted at the highest surface density. This shows that even though the protein immobilization on the surface is achieved successfully, functionality of the protein for virus detection after immobilization is questionable. Moreover, it is also seen from the figure that variability in DNA-tethered protein immobilized spots is very small. Hence, DDI is found to be an optimum technique for obtaining robust and reproducible protein microarrays.

These results also suggest that DDI technique can be easily adapted to immobilization of various proteins without a need for further optimizations (*see* **Note 15**).

3.4 SP-IRIS

1. SP-IRIS optical setup is based on a top-illumination microscope configuration. To create the optical path with the illuminating LED, 2-lens system is used and the LED is imaged onto the back aperture of the objective for Kohler illumination. LED light is first collimated with 30 mm-lens in the illumination path. Then, the collimated light gets focused onto the back focal aperture of the objective using a 50 mm-lens. Hence, the light beam is directed onto the sample stage which, then, gets reflected off the SP-IRIS sensor surface. With a beam splitter, the light beam is focused; therefore, it is directed down to the sample stage and the reflected light from the sensor surface is captured by the camera (*see* **Notes 16** and **17**).
2. Via the microscope objective, the light beam is focused.
3. After, the reflected light beam is collected by the objective and transmitted through the beam splitter.
4. The specular reflected light as well as the scatter light from the sample are focused via the tube lens onto the CCD camera where intensity image is recorded. The schematic representation of the system, light path and imaging principle are shown in Fig. 7. Figure 8 shows a representative image of the setup and its configuration.
5. For imaging, the microfluidic device is placed on the sample holder (stage) and endpoint images are taken.

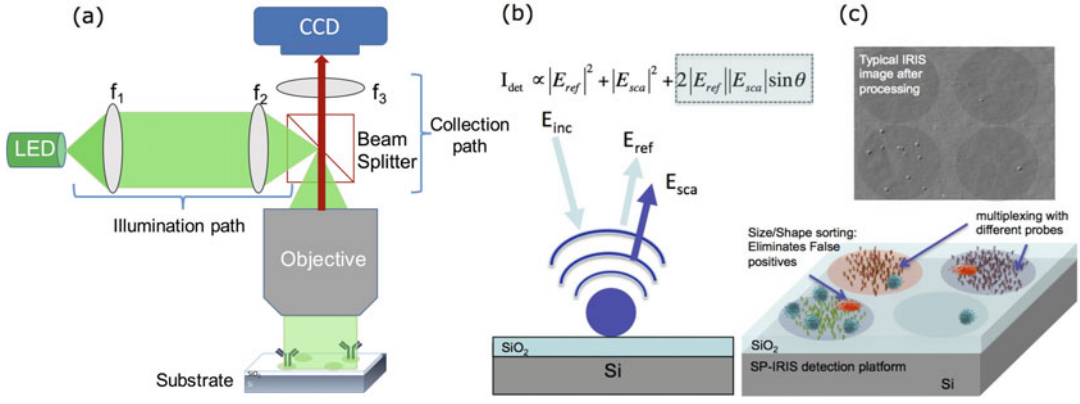

Fig. 7 (**a**) Schematic representation of the SP-IRIS setup. LED is used for illumination and bright field image is reflected on a CCD camera. (**b**) With the help of cross term (*highlighted*) in the equation, visibility of low-index nanoparticles is enabled with their enhanced intensity by order of magnitude compared to scattered intensity (middle term). (**c**) A representation of multiplexed SP-IRIS chip (*bottom*) and an actual image of detected particles on the chip after processing (*top*). Reprinted with permission from Avci et al. Sensors, 2015, 15, pp 17649–17665. 2016 Creative Commons (http:/creativecommons.org/licenses/by/4.0/)

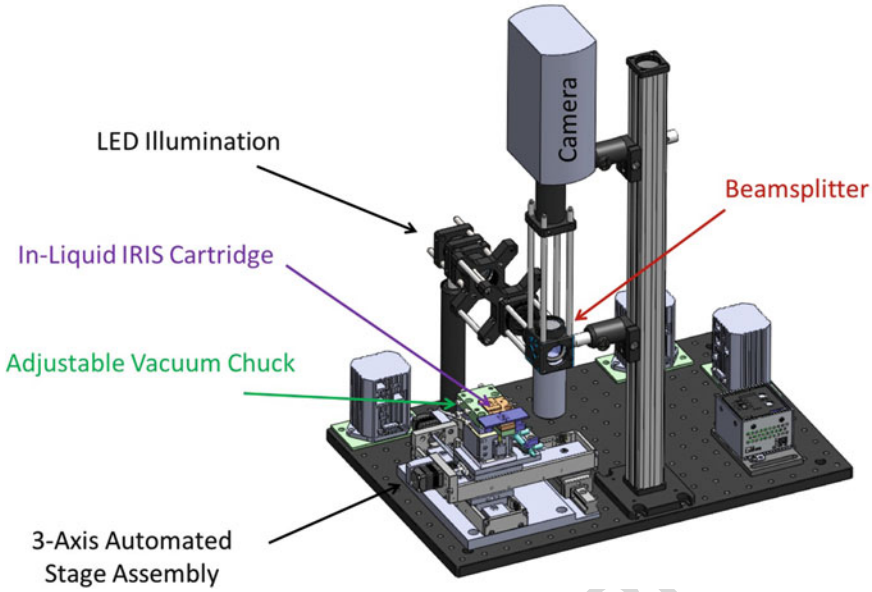

Fig. 8 Representative image of the SP-IRIS setup

3.5 Data Processing

1. Each spot is imaged in SP-IRIS.
2. The images for each spot are analyzed for bound virus particles.
3. By subtracting pre-incubation particle counts from post-incubation counts and dividing the result by the analyzed spot area, the net particle densities are determined (*see* **Note 18**).
4. Six spots for each condition are used to average the particle densities.
5. The morphological features as well as non-diffraction limited peaks are removed from the image with appropriate filters.
6. The signal coming from the particle is based on the interference between the scattered field from the particle and the reference field arising from the reflection off the sensor. The signal from the particle is normalized relative to the nearby background intensity. Custom particle detection software is developed in MATLAB to find particle-originated local intensity maxima which fall within the point spread function of the optical system (*see* **Note 19**).
7. The interaction of the light with small particle is considered as an induced dipole where its strength is proportional with the polarizability of the particle (α), as given in the following equation:

$$\alpha = 4\pi\varepsilon_0 r^3 \frac{\varepsilon_p - \varepsilon_m}{\varepsilon_p + 2\varepsilon_m} \quad (1)$$

where r is radius of the particle, ε_p and ε_m are particle and surrounding medium permittivity, respectively [20]. In interferometric imaging techniques, in the intensity recorded at the detector, strong reference field and weak scattered fields coming from the particle are mixed and can be expressed with the following equation:

$$I \propto |E_{ref}|^2 + |E_{sca}|^2 + 2|E_{ref}||E_{sca}| \cos\theta \quad (2)$$

In this equation, for weakly scattering particles, $|E_{sca}|^2$ is negligible. Hence, the signal is dominated by the cross term as seen in Fig. 7b. This signal appears as a dot in the image as seen in Fig. 7c. Based upon the contrast of the particle, the size is determined with the model. Since the virus particles scatter the light upon binding the surface, enhanced signal coming from the layered chip surface is detected on the CCD camera.

3.6 Single Particle Detection (In Liquid Virus Detection Measurements)

1. The flow cell is obtained by assembling the individual layers. The acrylic layer is placed as the base and then, biosensor chip is put in the middle of the cartridge. After placing the second layer, the third layer is placed on top providing imaging window like a polymer cover glass. Then, the fourth and fifth layers are placed and adaptors are attached to the fifth layer. FEP tubing is assembled to the adaptors. The syringe pump is connected via tubing to provide the flow. The flow is directed in the channels to the chip surface with the precisely designed microfluidic device as shown in Fig. 5.
2. The flow cell is placed on the sample stage of SP-IRIS underneath the objective for image acquisition. DNA-immobilized SP-IRIS chips are already placed in the microfluidic cartridges.
3. Acquisition software is opened and the camera is turned on.
4. Number of images to be averaged is determined and selected. Maximum exposure time before saturation of the camera is selected.
5. First, 13F6-DNA, B-conjugate is flowed at a concentration of 5 μg/mL in PBS with 1% BSA for 1 h to achieve protein immobilization on the chip.
6. To get pre-incubation particle counts in spots with different concentration of protein immobilized, SP-IRIS images are acquired.
7. Then, the chips are incubated with 10^4 PFU/mL EBOV-VSV by flowing it over the chip for 30 min.
8. After incubation, 400 μL sodium phosphate buffer is flowed over the microchannel and SP-IRIS images are acquired (*see* **Note 20**).

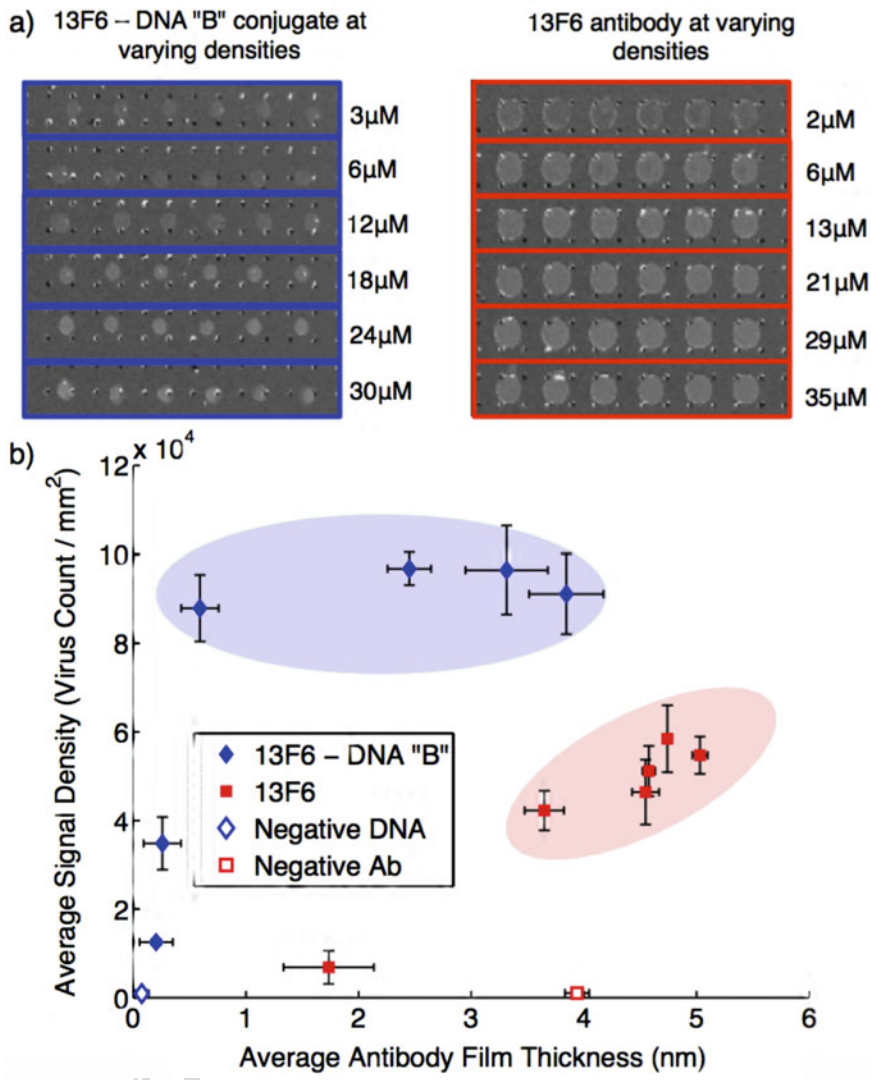

Fig. 9 (**a**) Left IRIS image showing different surface densities of immobilized antibody-DNA conjugate after hybridization of the B′ sequence with the 13F6-DNA "B" conjugate. *Right image* shows 13F6-antibody spots at different concentrations. (**b**) Effect of surface antibody density (1 nm = 1.2 ng/mm^2) on virus capture efficiency for both direct antibody and DNA-conjugated antibody immobilization. Average capture virus densities (n = 6 spots) obtained from SP-IRIS images versus average optical thickness of the antibody spots obtained from IRIS images were plotted. The *ellipses* indicate the range of surface antibody heights where the optimal virus capture occurs. Reprinted with permission from Seymour et al. Anal. Chem., 2015, 87 (20), pp. 10505–10512. Copyright 2016 American Chemical Society

9. Finally, end point images of virus-captured chips are acquired.
10. Figure 9 shows the comparison of the virus capture performance of both direct antibody-immobilized and DNA-directed-antibody immobilized assays. IRIS is used to show the surface morphologies of antibody and DNA-tethered

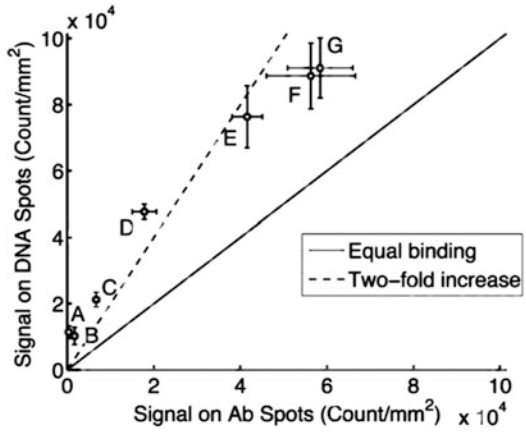

Experiment	Virus titer (PFU/ml)	Incubation time (min)	#-fold increase
A	$1x10^3$	60	34.3
B	$2x10^3$	15	6.1
C	$8x10^3$	15	3.2
D	$1x10^4$	15	2.7
E	$1x10^4$	30	1.8
F	$1x10^4$	30	1.6
G	$1x10^4$	30	1.6

Fig. 10 Comparing captured virus densities on direct-spotted and DNA-tethered antibodies from independently performed experiments. Each *letter* represents a data point next to it. Experimental conditions corresponding to A–G experiments are summarized in the table. Error bars show the variation between six spots for a given experiment. Reprinted with permission from Seymour et al. Anal. Chem., 2015, 87(20), pp 10505–10512. Copyright 2016 American Chemical Society

antibody spots at different concentrations. According to Fig. 9b, DNA-conjugated 13F6 performs optimally over a larger range of surface densities compared to the directly spotted antibody [19].

11. Figure 10 depicts the performance of the protein immobilization technique by varying the capture conditions. In general, since limited number of target is present at lower concentrations of the virus, a lower capture efficiency is obtained in both direct and DDI techniques. However, when the available targets increase in the solution, a drastic increase in DNA-tethered antibody microarray is observed; whereas, direct-antibody immobilized microarray does not show the same sensitivity. DDI makes the capture proteins highly available and accessible on the sensor surface. Hence, an improved binding capacity is achieved in shorter time.

4 Notes

1. Adjusting the NA offers a tradeoff between nanomaterial contrast and usable field of view (FOV).
2. Oxide thicknesses are chosen to maximize the phase angle term.
3. It can be synthesized as described in the reference [21]. One of the most affecting components of protein microarrays is microarray immobilization surface. For DDI technique, specifically a reactive-functional surface is needed in order to achieve the

covalent attachment of the surface probe DNA sequences to the sensor surface. Therefore, MCP-2 is an excellent option for this purpose. It bears functional NHS groups which take part in covalent immobilization of the amino-modified oligonucleotides. Moreover, due to its unique 3D structure, it provides right confirmation for oligonucleotides by enhancing immobilization with its hydrophobic regions. Also, MCP-2 lowers non-specific bindings of proteins providing a perfect sensor surface for sensitive and selective detections [22].

4. NHS groups are active for further possible reactions. Therefore, it is important to block them after the completion of immobilization. Otherwise, it may cause further crosslinking; thus, a decrease in the efficiency in protein immobilization due to the less availability of the probes or proteins.
5. Antibody spots directly immobilized for comparison purpose only require antibody spotting buffer (1×): 1× PBS with a final concentration of 25 mM trehalose, pH 7.5. 1.420 g of Na_2HPO_4 and 0.245 g of NaH_2PO_4 is dissolved in 1 L of filtered deionized water. pH is adjusted to 7.5 with HCl. 8.557 g of trehalose is dissolved in filtered deionized water to have 25 mM trehalose solution. Both stored at room temperature.
6. 5′-polyA sequence is added as a spacer to DNA sequence which is conjugated to the antibody.
7. It is important to use a plastic petri dish in the polymer coating process of the chips. Since a glass petri dish competes with the chip in functionalization, for higher coating efficiency, a plastic petri dish is used.
8. It is critical to store the functionalized chips in a desiccator after fabrication. The chips can be stored in the desiccator for up to 3 weeks under vacuum. It would be worthwhile to bake the chips at 80 °C for 15 min in a vacuum oven prior to use in order to have completely dried and NHS-active polymer coating on the chips for successive spotting.
9. Surface antibody density is an important criterion which drastically affects assay sensitivity. Surface density of the antibodies should be optimized for a given application to optimize the target capture.
10. During spotting of DNA, it is very important to keep the humidity at an optimum level in the spotter chamber. The optimal level we found is 67% for the humidity. After spotting, the chips are kept in the spotter chamber at 67% humidity overnight. However, for antibody spotting, optimum spotting is found as 57–59%. These changes in the humidity make huge variations in the spot morphology. If DNA is spotted at the

same humidity with antibody, then, a smaller and non-uniform spot morphology is observed.

11. DNA concentration is optimized to obtain 1–2 DNA sequences per antibody. After conjugation, yield of reaction is determined by Bradford assay. The monoclonal antibody is conjugated to DNA sequence, B′, in 1:1.5 ratio. 13F6-DNA, B, is antibody-conjugates against Ebola-GP pseudotyped VSV.
12. Different antibodies have different probe characteristics. Therefore, in order to obtain a uniform spot morphology and surface density, for each type of protein, an optimization study is needed. This is not time and cost efficient. On the other hand, oligonucleotides only differ in sequences and length among each other; therefore, as long as the length of the sequence is kept constant, DNA immobilization characteristics generally stay the same. DNA spotting does not depend on the type or immobilization. Hence, a standard and parameter-independent protein immobilization can be achieved with DDI. Thereupon, this technique is preferred in this study.
13. Antibody spots directly immobilized for comparison purpose only. (a) Antibody solutions are prepared as 3 mg/mL in antibody spotting buffer. The humidity during spotting is kept between 57 and 59%. The spotted chips are kept in the spotter chamber at 67% humidity overnight. (b) To evaluate the effect of antibody immobilization density on the virus capture, anti-EBOV GP antibody (13F6) is spotted at varying concentrations on SP-IRIS substrates (5, 4, 3, 2 ,1 and 0.5 mg/mL).
14. IRIS has a different modality of operation. The important difference between IRIS and SP-IRIS is the magnification of the optical system. In IRIS, numerical aperture of the objective lens is different. Hence, low-magnification can be achieved; whereas, using SP-IRIS, high-magnification is achieved. This modality is based on spectral reflectivity. When the biomass accumulates on the sensor surface, the thickness on the sensor increases. This increase generates a quantifiable change in the spectral reflectivity depending on the optical path difference (OPD) between substrate surface and biomass accumulated substrate surface. With the help of low-magnification modality, multiplexed monitoring of biomolecule immobilization or capture can be precisely acquired. Therefore, using IRIS, a larger field of view (FOV), approximately 1 in.^{2}, can be captured. Hence, IRIS can be used for quality control of the assay chips [20]. Variations in the probe immobilization can be detected easily.
15. Spot morphology is another important criterion for single particle detection. It directly affects probe density, capture

efficiency; thus, the reproducibility in the experiments. Non-uniform spot morphology causes spot-to-spot and assay-to-assay changes. Capture efficiency is directly proportional with the surface probes. A destroyed morphology causes non-binding of the target particle; therefore, false negative results may be obtained in quantification of the signal [23]. These irregularities may be crystallization appearing as bright spots in the image, coffee rings in the outer region of the spot or aggregations causing non-uniform regions in the spot. The detector response should not depend on the parameters. However, when antibodies are used as the surface probe, a robust microarray design may not always be achieved due to the problems in consistency in the spot morphology. On the other hand, DNA spotting is always uniform. More robust protein microarrays can be achieved via DDI. DNA spot morphology stays almost identical in repetitive spotting which provides a uniformity in the sensor response among spot-to-spot and assay-to-assay measurements.

16. The significant parameters in the optical setup are the illumination wavelength, uniformity, NA, magnification and camera pixel size. These parameters affect the resolution and the accuracy of sample sizing. In addition, since sample sizing is determined using the contrast of the central peak to near-neighbor background pixels; improper and non-uniform illumination cause sizing obscurity. Kohler illumination is implemented in the optical system due to its superiority over critical illumination.
17. To achieve a uniform illumination, a diffuser is placed in front of the LED light source.
18. In order to minimize signal variations arising from the spot morphology, it is desirable to take a pre-incubation image to later subtract from the post-incubation image to calculate the net number of bound particles.
19. Other image processing software such as ImageJ can be used as an alternative to MATLAB for post-processing and quantification.
20. During the microarray preparation processes, especially in between washings, the chips should always be wetted. Extra care should be taken.

References

1. MacBeath G, Schreiber SL (2000) Printing proteins as microarrays for high-throughput function determination. Science 289:1760–1763
2. Sun H, Chen GYJ, Yao SQ (2013) Recent advances in microarray technologies for proteomics. Chem Biol 20:685–699

3. Hall DA, Tacek J, Snyder M (2007) Protein microarray technology. Mech Ageing Dev 128 (1):161–167
4. Avci O, Lortlar ÜN, Yalcin A et al (2015) Interferometric Reflectance imaging sensor (IRIS)-a platform technology for multiplexed diagnostics and digital detection. Sensors 15 (7):17649–17665
5. Schwenk JM, Lindberg J, Sundberg M et al (2007) Determination of binding specificities in highly multiplexed bead-based antibody assays for antibody proteomics. Mol Cell Proteomics 6:125–132
6. Cretich M, Daaboul GG, Sola L et al (2015) Digital detection of biomarkers assisted by nanoparticles: application to diagnostics. Trends Biotechnol 33(6):343–351
7. Yurt A, Daaboul GG, Connor JH et al (2012) Single nanoparticle detectors for biological applications. Nanoscale 4(3):715–726
8. Walt D (2013) Optical methods for single molecule detection and analysis. Anal Chem 85 (3):1258–1263
9. Daaboul GG, Lopez CA, Chinnala J et al (2014) Digital sensing and sizing of vesicular stomatitis virus pseudotypes in complex media: a model for ebola and marburg detection. ACS Nano 8(6):6047–6055
10. Monroe MR, Daaboul GG, Tuysuzoglu A et al (2013) Single nanoparticle detection for multiplexed protein diagnostics with attomolar sensitivity in serum and unprocessed whole blood. Anal Chem 85(7):3698–3706
11. Sevenler D, Lortlar ÜN, Ünlü MS (2015) Nanoparticle biosensing with interferometric reflectance imaging. In: Vestergaard MC, Kerman K, Hsing I-M, Tamiya E (eds) Nanobiosensors and nanobioanalyses. Springer, Tokyo, pp 81–95
12. Monroe MR, Reddington A, Collins AD et al (2011) Multiplexed method to calibrate and quantitate fluorescence signal for allergen-specific IgE. Anal Chem 83(24):9485–9491
13. Niemeyer CM, Boldt L, Ceyhan B et al (1999) DNA-directed immobilization: efficient, reversible, and site-selective surface binding of proteins by means of covalent DNA-streptavidin conjugates. Anal Biochem 268:54–63
14. Ladd J, Boozer C, Yu Q et al (2004) DNA-directed protein immobilization on mixed self-assembled monolayers via a streptavidin bridge. Langmuir 20:8090–8095
15. Schroeder H, Adler M, Gergk K et al (2009) User configurable microfluidic device for multiplexed immunoassays based on DNA-directed assembly. Anal Chem 81:1275–1279
16. Washburn AL, Gomez J, Bailey RC (2011) DNA-encoding to improve performance and allow parallel evaluation of the binding characteristics of multiple antibodies in a surface-bound immunoassay format. Anal Chem 83:3572–3580
17. Wacker R, Niemeyer CM (2004) DNA- µFIA-a readily configurable microarray-fluorescence immunoassay based on DNA-directed immobilization of proteins. Chem Bio Chem 5:453–459
18. Wacker R, Schroder H, Niemeyer CM (2004) Performance of antibody microarrays fabricated by either DNA-directed immobilization, direct spotting, or streptavidin-biotin attachment: a comparative study. Anal Biochem 330:281–287
19. Seymour E, Daaboul GG, Zhang X et al (2015) DNA-directed antibody immobilization for enhanced detection of single viral pathogens. Anal Chem 87(20):10505–10512
20. Avci O, Adato R, Yalcin OA et al (2016) Physical modeling of interference enhanced imaging and characterization of single nanoparticles. Opt Express 24(6):6094–6114
21. Pirri G, Damin F, Chiari M et al (2004) Characterization of the polymeric adsorbed coating for DNA microarray glass slides. Anal Chem 76 (4):1352–1358
22. Yalçin A, Damin F, Özkumur E et al (2009) Direct observation of conformation of a polymeric coating with implications in microarray applications. Anal Chem 81(2):625–630
23. Romanov V, Davido SN, Miles AR et al (2014) A critical comparison of protein microarray fabrication technologies. Analyst 139 (6):1303–1326